Inorganic Chemistry

Article

pubs.acs.org/IC

Ferrocene-Based Tetradentate Schiff Bases as Supporting Ligands in Uranium Chemistry

Clément Camp,[†,§] Lucile Chatelain,[†,§,‡] Victor Mougel,[†,§] Jacques Pécaut,[†,§] and Marinella Mazzanti*[,‡]

[†]Univ. Grenoble Alpes, INAC-LCIB, RICC, and [§]CEA, INAC-LCIB F-38000 Grenoble, France

[‡]Institut des Sciences et Ingénierie Chimiques, Ecole Polytechnique Fédérale de Lausanne (EPFL), CH-1015 Lausanne, Switzerland

Supporting Information

ABSTRACT: Uranyl(VI), uranyl(V), and uranium(IV) complexes supported by ferrocene-based tetradentate Schiff-base ligands were synthesized, and their solid-state and solution structures were determined. The redox properties of all complexes were investigated by cyclic voltammetry. The bulky salfen-^{t}Bu$_2$ allows the preparation of a stable uranyl(V) complex, while a stable U(IV) bis-ligand complex is obtained from the salt metathesis reaction between $[UI_4(OEt_2)_2]$ and K_2salfen. The reduction of the $[U(salfen)_2]$ complex leads to an unprecedented intramolecular reductive coupling of the Schiff-base ligand resulting in a C−C bond between the two ferrocene-bound imino groups.

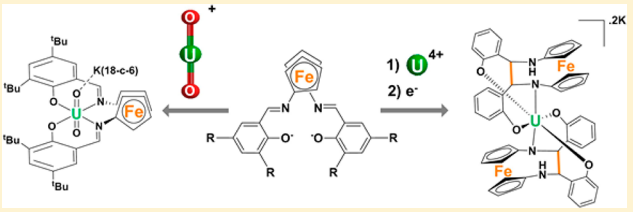

INTRODUCTION

Ligand design has played a crucial role in the recent advancements witnessed in uranium chemistry. Notably, the choice of the ancillary ligand is particularly crucial in the stabilization of highly reactive species and unusual oxidation states,[1,2] in promoting original reactivity[3,4] and implementing magnetic properties.[5,6]

Tetradentate ONNO Schiff-base ligands have extensively been used as supporting ligands in d-block chemistry because of their ability to stabilize metals in various oxidation states. Surprisingly, the use of Schiff bases as ancillary ligands in uranium chemistry remains limited for oxidation states lower than (VI).[7] Notably, only a very few examples of U(IV)[8] and U(III)[9,10] complexes of Schiff bases have been reported so far. Only in recent years, Schiff bases have been increasingly used as effective ligands for the stabilization of uranium in the elusive oxidation state of +V.[11] Our group has reported the synthesis of several stable mononuclear and polynuclear uranyl(V)[11c−g] complexes, which have proven to be attractive building blocks in the design of actinide-based molecular magnets.[6b,12] The structure and electronic properties of the Schiff-base ligand have proven crucial for the stabilization of uranyl(V) with respect to the disproportionation reaction to UO_2^{2+} and U(IV).[11b,d] In addition, our group has also shown that Schiff bases could be used to promote ligand-centered multielectron redox reactivity in U(IV) species.[8a,13] Notably the reduction of U(IV) salophen (salophen = *N*,*N*′-disalicylidene-*o*-phenylenediaminate) complexes promote C−C bond formation to afford dinuclear or mononuclear U(IV) amido complexes (Scheme 1) that can release up to four electrons to substrates through the oxidative cleavage of the C−C bond.

The redox properties of such ligand-centered redox-active U(IV) systems should be easily tuned by straightforward changes on the Schiff-base scaffold involving either the phenol substituents or the diimine bridging moiety.[14] In this context, ferrocene-based Schiff-base ligands such as salfen^{2-} (Figure 1) are an attractive class of redox-active ligands because they associate two different redox-active fragments on the same ligand (imino group and ferrocene). Notably, the capability of the ferrocene unit to participate in redox events might increase the reactivity possibilities of their complexes. Moreover, compared to the salophen platform, the length of the spacer fragment (1,1′-ferrocenyl vs 1,2-phenyl bridge) is increased, providing a larger ONNO cavity well-suited for uranium.

1,1′-disubstituted ferrocene-based ligands have proven versatile supporting ligands in the chemistry of group 3 elements and uranium due to the flexibility and redox-active

Scheme 1. Reductive Coupling of the Salophen Ligand in Uranium Chemistry

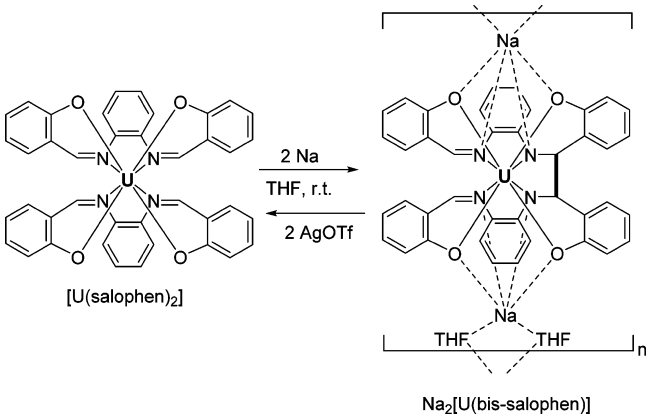

Received: February 27, 2015
Published: May 26, 2015

DOI: 10.1021/acs.inorgchem.5b00467
Inorg. Chem. 2015, 54, 5774−5783

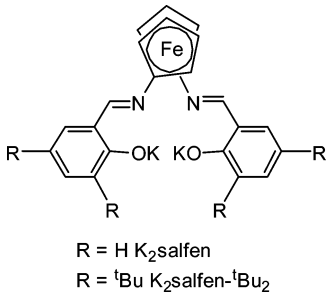

Figure 1. Representation of salfen ligands.

character of ferrocene, leading to effective catalysts, to novel reactivity, and to effective intermetallic electronic communication between iron and the metal center.[15,16] However, the coordination chemistry of the ferrocene-based Schiff-base salfen ligand remains practically unexplored with only three reports on the use of this Schiff-base ligand in combination with Mg(II),[17] Zr(IV),[17] Ti(IV),[17] Ce(III),[18] Ce(IV),[19] and Y-(III).[18,19] In view of the high steric and electronic flexibility of these ligands we set out to explore its ability to stabilize unusual uranium oxidation states and to support ligand-centered multielectron redox chemistry in uranium-containing compounds. Here we report the synthesis, characterization, and redox properties of salfen complexes of uranium in different oxidation states.

EXPERIMENTAL SECTION

General Considerations. Unless otherwise noted, all manipulations were performed at ambient temperature under an inert argon atmosphere using Schlenk techniques and an MBraun glovebox equipped with a purifier unit. The water and oxygen levels were always kept lower than 1 ppm. Glassware was dried overnight at 130 °C before use and dried in vacuo. ^{1}H NMR experiments were performed using NMR tubes adapted with J. Young valves. ^{1}H NMR spectra were recorded on Bruker 200 and 500 MHz and Varian Mercury 400 MHz spectrometers. NMR chemical shifts are reported in parts per million with solvent as internal reference. Elemental analyses were performed under argon by Analytische Laboratorien GMBH at Lindlar, Germany.

Starting Materials. Unless otherwise noted, reagents were purchased from commercial suppliers and used without further purification. The solvents were purchased from Aldrich or Eurisotop (deuterated solvents) in their anhydrous form, conditioned under argon and vacuum distilled from K/benzophenone (toluene, hexane, pyridine (Py), and tetrahydrofuran (THF)). All solid reagents were dried under high vacuum for 7 d prior to use. $[UO_2I_2(Py)_3]$,[1d] $\{[(UO_2(Py)_5)][(KI_2(Py)_2)]\}_n$,[1d11c] $[UI_4(OEt_2)_2]$,[20] and $[UI_3(THF)_4]$[21] were prepared according to the published procedures. The H_2salfen and H_2salfen-^{t}Bu$_2$ ligands and the K_2salfen and $[K(THF)]_2$(salfen-^{t}Bu$_2$) ligand salts were prepared according to the published procedures.[17,19]

Caution! *Depleted uranium (primary isotope ^{238}U) is a weak α-emitter (4.197 MeV) with a half-life of 4.47 × 10^9 years. Manipulations and reactions should be performed in monitored fume hoods or in an inert atmosphere glovebox in a radiation laboratory equipped with α-counting equipment.*

Synthesis of [UO$_2$(salfen-^{t}Bu$_2$)], 1. A red solution of $[UO_2I_2(Py)_3]$ (10.0 mg, 0.013 mmol, 1 equiv) in pyridine (0.5 mL) was added to a light red solution of K_2salfen-^{t}Bu$_2$.$(THF)_2$ (9.5 mg, 0.013 mmol, 1 equiv) in pyridine (0.5 mL), yielding, after 30 min of stirring, a dark red solution with an off-white precipitate. The off-white precipitate was removed by filtration. Slow diffusion of hexane (one week) into this solution afforded the desired compound as a red crystalline solid (11 mg, 0.011 mmol, 90% yield). ^{1}H NMR (200 MHz, Py-d_5, 298 K): δ = 10.12 (s, 2H), 8.10 (d, 2H), 7.70 (d, 2H), 4.76 (t, 4H), 4.63 (t, 4H), 2.03 (s, 18H), 1.41 (s, 18H). Electrospray ionization mass spectrometry (ESI-MS): m/z = 955.3 ($[UO_2$(salfen-^{t}Bu$_2$)]K$^+$). Anal. Calcd for $[UO_2$(salfen-^{t}Bu$_2$)]·0.15KI $C_{40}H_{50}FeN_2O_4UK_{0.15}I_{0.15}$: C, 51.02; H, 5.35; N, 2.98. Found: C, 50.99; H, 5.75; N, 3.09%.

Synthesis of [UO$_2$(salfen-^{t}Bu$_2$)(K18-c-6)], 2. A solution of K_2salfen-^{t}Bu$_2$·$(THF)_{0.31}$ (71.5 mg, 0.096 mmol, 1 equiv) in pyridine (2 mL) was added to an orange suspension of $\{[(UO_2(Py)_5)]$-$[KI_2(Py)_2]\}_n$ (106.9 mg, 0.096 mmol, 1 equiv) in pyridine (0.5 mL). A colorless solution of 18-c-6 (75.9 mg, 0.290 mmol, 3 equiv) in pyridine (2 mL) was then added to the reaction mixture resulting in a dark red solution. The solution was stirred 30 min at room temperature and concentrated to 1 mL. This solution was filtered, and hexane (6 mL) was added to the filtrate, resulting in the formation of a brown precipitate. The solid was recovered by filtration, washed with hexane (1 mL), and dried under vacuum to afford $[UO_2$(salfen-^{t}Bu)(K18-c-6)]·0.8hexane. (52.9 mg, 45% yield). Anal. Calcd for $[UO_2$(salfen-^{t}Bu)(K18-c-6)]·0.8hex $C_{56.8}H_{85.2}KFeN_2O_{10}U$: C, 52.92; H, 6.66; N, 2.17. Found: C, 52.89; H, 6.93; N, 2.34%. Orange single crystals of **2** suitable for X-ray diffraction were obtained after two weeks by recrystallization from toluene at room temperature. ^{1}H NMR of **2** (500 MHz, Py-d_5, 323 K): δ = 6.89 (s, 2H), 6.64 (s, 2H), 5.23 (s, 2H), 4.65 (s, 24H, 18-c-6), 4.27 (s, 4H), 1.09 (s, 4H), 0.77 (s, 18H), −3.41 (s, 18H). ESI-MS: m/z = 1522.2 ($[UO_2$(salfen-^{t}Bu$_2$)(K18-c-6)](K18-c-6)$^+$).

Reaction of K$_2$salfen with $\{[(UO_2(Py)_5)][KI_2(Py)_2]\}_n$. A solution of K_2salfen (10.0 mg, 0.018 mmol, 1 equiv) in pyridine (1 mL) was added to an orange suspension of $\{[(UO_2(Py)_5][KI_2(Py)_2]\}_n$ (20.2 mg, 0.018 mmol, 1 equiv) in pyridine (1 mL), resulting in a dark red solution. The solution was stirred over 15 min. Analysis of the crude reaction mixture by ^{1}H NMR revealed the presence of the signals of $[U(salfen)_2]$ and of $[UO_2(salfen)]$. Complete disproportionation was achieved in 12 h.

Synthesis of [U(salfen)$_2$], 3. A solution of K_2salfen (50.0 mg, 0.099 mmol, 2 equiv) in THF (4 mL) was added to a red solution of $[UI_4(OEt_2)_2]$ (44.1 mg, 0.049 mmol, 1 equiv) in THF (4 mL). The resulting red suspension was stirred for 12 h at room temperature before filtration. The resulting red filtrate was evaporated to dryness to give $[U(salfen)_2]$·0.2 KI as a red powder (40.8 mg, 0.037 mmol, 75% yield). Single crystals suitable for X-ray diffraction were obtained by slow diffusion of diisopropyl ether into a THF solution of $[U(salfen)_2]$. ^{1}H NMR (200 MHz, THF-d_8, 298 K): δ = 23.5 (s, 4H), 17.6 (t, 4H), 12.8 (d, 4H), 12.2 (t, 4H), 10.6 (s, 4H), 3.6 (s, 4H), −2.9 (s, 4H), −7.6 (s, 4H), −19.0 (s, 4H). ^{1}H NMR (200 MHz, py-d_5, 298 K): δ = 23.9 (s, 4H), 17.8 (t, 4H), 12.9 (d, 4H), 12.3 (t, 4H), 10.7 (s, 4H), 4.1 (s, 4H), −2.6 (s, 4H), −7.6 (s, 4H), −19.0 (s, 4H). Anal. Calcd for $[U(salfen)_2]$·0.2(KI) $C_{48}H_{36}Fe_2N_4O_4UK_{0.2}I_{0.2}$: C, 51.67; H, 3.25; N, 5.02. Found: C, 51.70; H, 3.48; N, 4.96%.

Reaction of K$_2$salfen with [UI$_3$(THF)$_4$]. A solution of K_2salfen (7.5 mg, 0.010 mmol, 1 equiv) in THF-d_8 (0.5 mL) was added to a blue solution of $[UI_3(THF)_4]$ (5.0 mg; 0.010 mmol, 1 equiv) in THF-d_8 (0.5 mL). The resulting brown suspension was stirred for 1 h at room temperature, and the solids were removed by filtration. The ^{1}H NMR spectrum of this solution shows that $[U(salfen)_2]$ is obtained as the unique salfen-containing species.

Reduction of [U(salfen)$_2$]. A solution of K_2salfen (50.0 mg, 0.099 mmol, 2 equiv) in THF (4 mL) was added to a red solution of $[UI_4(OEt_2)_2]$ (44.1 mg, 0.049 mmol, 1 equiv) in THF (4 mL). The resulting red suspension was stirred for 30 min at room temperature. To the resulting red-orange suspension was added KC_8 (26.5 mg, 0.196 mmol, 4.0 equiv), and the mixture was stirred at room temperature for 2 h. This afforded a dark brown suspension. The solid residues were removed by centrifugation. The ^{1}H NMR spectrum of the supernatant showed the formation of mixture of K_3[U(bis-salfen)(Hbis-salfen)] **4-H** and K_2[U(Hbis-salfen)$_2$] **4-H$_2$**. Attempts to separate the two species by crystallization were unsuccessful. While the reduction gives reproducibly a mixture of the **4-H** and **4-H$_2$**, the isolation of each of these species in analytically pure form was not possible.

A few single crystals of **4-H** suitable for X-ray diffraction were grown by slow diffusion of diisopropyl ether into this solution. While

DOI: 10.1021/acs.inorgchem.5b00467
Inorg. Chem. 2015, 54, 5774−5783

the quality of the structure is not sufficient for a discussion of the metrical parameters, the connectivity clearly shows the presence of a complex of formula K_3[U(bis-salfen)(Hbis-salfen)] ; space group $P2_1/a$; a = 20.5937(13) Å, b = 31.3962(15) Å, c = 25.6297(12) Å, $\alpha = \beta = 90°$, γ = 108.864(6)°.

Spectroscopic data performed on isolated crystals of K_3[U(bis-salfen)(Hbis-salfen)] **4-H**: ESI-MS: m/z = 1201.0 $[M + H]^+$. ^{1}H NMR (200 MHz, THF-d_8, 298 K): δ = 36.4 (d, 1H), 32.3 (d, 1H), 30.5 (d, 1H), 27.5 (d, 1H), 21.0 (t, 1H), 17.3 (d, 1H), 16.2 (d, 1H), 15.7 (d, 1H), 13.6 (d, 1H), 12.1 (s, 1H), 10.4 (s, 1H), 10.1 (s, 1H), 9.6 (t, 1H), 9.3 (t, 1H), 9.1 (t, 1H), 9.0 (t, 1H), 7.0 (t, 1H), 6.8 (t, 1H), 6.4 (t, 1H), 6.1 (t, 1H), 4.5 (s, 1H), 3.4 (s, 1H), 3.3 (s, 1H), 2.5 (s, 1H), 2.1 (s, 1H), 2.0 (d, 1H), 1.5 (s, 1H), 0.4 (s, 1H), 0.3 (d, 1H), −1.5 (d, 1H), −1.7 (s, 1H), −2.6 (s, 1H), −3.0 (s, 1H), −23.2 (s, 1H), −26.6 (s, 1H), −27.5 (s, 1H).

Spectroscopic data for K_2[(Hbis-salfen)$_2$] **4-H$_2$** obtained from a reaction mixture after partial separation: ^{1}H NMR (200 MHz, THF-d_8, 298 K): δ = 19.7 (d, 2H), 13.5 (t, 2H), 13.0 (d, 2H), 11.7 (t, 2H), 10.4 (t, 2H), 9.6 (t, 2H), 9.2 (d, 2H), 8.0 (d, 2H), −2.7 (s, 2H), −3.1 (s, 2H), −3.3 (s, 2H), −5.3 (s, 2H), −6.1 (s, 2H), −6.9 (s, 2H), −12.0 (s, 2H), −13.1 (s, 2H), −16.8 (s, 2H), −19.1 (brs, 2H).

Single crystals of [(K18-c-6)$_2$U(bis-salfen)(Hbis-salfen)]$_2$(K18-c-6)$_2$·7thf, **5**, suitable for X-ray diffraction were grown by slow diffusion of diisopropyl ether into the THF reaction mixture in the presence of 18-c-6.

Single crystals of [K(dibenzo18-c-6)(py)]$_2$[U(Hbis-salfen)$_2$]·py$_5$, **6** suitable for X-ray diffraction were grown by slow diffusion of hexane into a pyridine solution of the complex reaction mixture in the presence of excess dibenzo18-c-6.

Oxidation of 4H and 4H$_2$. A red solution of [U(salfen)$_2$] **3** (6.0 mg, 0.006 mmol, 1 equiv) in THF-d_8 (0.7 mL) was added to solid KC_8 (3 mg, 0.022 mmol, 4.0 equiv) at room temperature. To the resulting dark brown suspension of a mixture of K_3[U(bis-salfen)(Hbis-salfen)] **4-H** and K_2[U(Hbis-salfen)$_2$] **4-H$_2$** was added solid AgOTf (5.7 mg, 0.022 mmol, 4.0. equiv) affording a red solution and a black solid. ^{1}H NMR spectra were recorded at each step, and integrals were compared to an internal reference (toluene). The addition of 4 equiv of AgOTf allows a complete conversion of the mixture of reduced species into the initial [U(salfen)$_2$] complex.

Electrochemical Methods. Cyclic voltammetry experiments were performed at room temperature in an argon-filled glovebox described above. Data were collected using a Biologic SP-300 potentiostat. All samples were 2−6 mM in complex with 0.1 M $[Bu_4N][PF_6]$ supporting electrolyte in pyridine solution. The experiments were performed with a platinum disk (d = 5 mm) working electrode, a platinum wire counter electrode, and a Ag/AgCl reference electrode. The experiments were repeated on independently synthesized samples to assess the reproducibility of the measurement. Potential calibration was performed at the end of each data collection cycle using the ferrocene/ferrocenium $[(C_5H_5)_2Fe]^{+/0}$ couple as an internal standard.

Magnetic Methods. Static magnetic properties were measured using a Quantum Design SQUID MPMS-XL 5.0 susceptometer. Ultra-Low Field Capability (0.05 G for the 5 T magnets. Continuous Low Temperature Control/Temperature Sweep Mode (CLTC) − Sweep rate: 0.001−10 K/min. The samples were pressed under argon and blocked from torquing using eicosane into a 5 mm Suprasil-Quartz tube, which was then sealed under vacuum. Contribution to the magnetization from the empty Suprasil-Quartz tube was measured independently and subtracted from the total measured signal. Diamagnetic corrections were made using Pascal's constants.

X-ray Crystallography. Diffraction data were taken using an Oxford-Diffraction XCallibur S kappa geometry diffractometer (Mo Kα radiation, graphite monochromator, λ = 0.710 73 Å). To prevent evaporation of cocrystallized solvent molecules the crystals were coated with light hydrocarbon oil, and the data were collected at 150 K. The cell parameters were obtained with intensities detected on three batches of five frames. The crystal-detector distance was 4.5 cm. The number of settings and frames has been established taking in consideration the Laue symmetry of the cell by CrysAlisPro Oxford-diffraction software.[22] 225 for **1**, 491 for **2**, 964 for **3**, 500 for **5**, and 1009 for **6** narrow data were collected for 1° increments in ω with a 40 s exposure time for **1**, 180 s for **2**, 10 s for **3**, 1 s for **5**, and 4 s for **6**. Unique intensities detected on all frames using the Oxford-diffraction Red program were used to refine the values of the cell parameters. The substantial redundancy in data allows empirical absorption corrections to be applied using the ABSPACK Oxford-diffraction program[22] for **1** and **6**, and analytical absorption correction for **2**, **3**, and **5**. Space groups were determined from systematic absences, and they were confirmed by the successful solution of the structure. The structures were solved by direct methods using the SHELXTL 6.14 package or by charge flipping method using superflip. All non-hydrogen atoms were found by difference Fourier syntheses and refined on F^2. For **3** hydrogen atoms were found by Fourier syntheses except for interstitial solvent H atoms, which were fixed in ideal position. For **1**, **2**, **5**, and **6** hydrogen atoms were fixed in ideal position. Full crystallographic details are given in Supporting Information, Table S.1.

RESULTS AND DISCUSSION

Uranyl Complexes. The uranyl (VI) complex [UO_2(salfen-^{t}Bu$_2$)], **1**, was prepared from the salt metathesis reaction between K_2salfen-^{t}Bu$_2$ and [UO_2I_2(Py)$_3$][1d] in pyridine (Scheme 2). The ^{1}H NMR spectrum recorded for a pyridine solution of **1** features seven resonances in the diamagnetic region, as expected for a symmetric f^0 uranyl(VI) compound with one low-spin Fe(II) center.

Scheme 2. Synthesis of the Uranyl Complexes [UO_2(salfen-^{t}Bu$_2$)] 1 and [UO_2(salfen-^{t}Bu$_2$)(K18-c-6)] 2

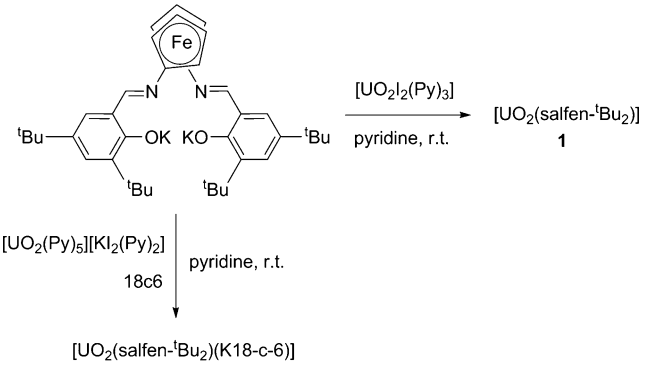

The reaction of the uranyl(V) precursor {[(UO_2(Py)$_5$)]-[KI_2(Py)$_2$]}$_n$[1d] with K_2salfen-^{t}Bu$_2$ in pyridine led to the formation of a stable uranyl(V) complex as suggested by the paramagnetically shifted ^{1}H NMR spectrum, which displays a single set of seven resonances between 6.83 ppm and −3.87 ppm in pyridine (Supporting Information, Figure S.5). The stable uranyl(V) complex [UO_2(salfen-^{t}Bu$_2$)(K18-c-6)], **2**, is isolated in the presence of 18-c-6 (Scheme 2). The proton NMR spectrum recorded for a pyridine solution of **2** (Supporting Information, Figure S.7) shows seven paramagnetically shifted signals for the salfen-^{t}Bu$_2$ ligand, in agreement with the presence of a uranyl(V) C_{2v} symmetric complex. ^{1}H NMR studies show that complex **2** is highly stable with respect to the disproportionation for at least 20 d in pyridine solution (see Supporting Information).

Note that the reaction of the uranyl(V) precursor {[(UO_2(Py)$_5$)][KI_2(Py)$_2$]}$_n$[1d] with K_2salfen in pyridine leads, after formation of a transient uranyl(V) species, to disproportionation of uranyl(V) resulting in the formation of a mixture of U(IV) and UO_2^{2+} species from which we identified the presence of the [U(salfen)$_2$] and [UO_2(salfen)] complexes

DOI: 10.1021/acs.inorgchem.5b00467
Inorg. Chem. 2015, 54, 5774−5783

(Supporting Information, Figure S.4). The disproportionation is complete after 12 h.

This highlights the important role of the steric hindrance provided by the bulky *tert*-butyl groups on the phenol arms in preventing the disproportionation of uranyl(V) in the $[UO_2(salfen\text{-}^tBu_2)(K18\text{-}c\text{-}6)]$ complex. The disproportionation of uranyl(V) is believed to occur through the formation of UO_2^+–UO_2^+ cation–cation dimeric species. The presence of bulky groups probably prevents the formation of such dimeric cation–cation intermediates by hindering the coordination to the uranium center of the uranyl(V) oxo group. Similar behavior was previously observed with tetradentate Schiff-base salophen and aminophenolate supporting ligands.[11c,23]

The solid-state crystal structures of complexes **1** and **2** were determined by X-ray diffraction studies and are presented in Figures 2 and 3, respectively. The crystal structure of **2** shows

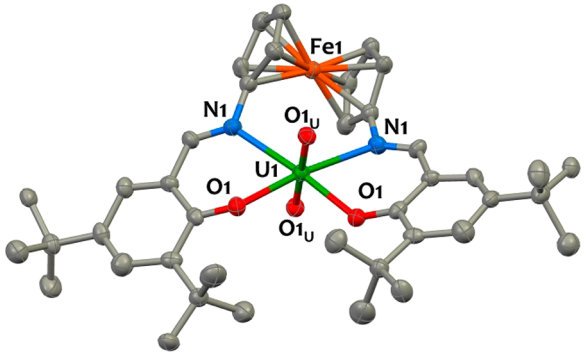

Figure 2. Solid-state molecular structure of $[UO_2(salfen\text{-}^tBu_2)]$ **1**. Hydrogen atoms and solvent molecules are omitted for clarity. Uranium (green), iron (orange), nitrogen (blue), oxygen (red), and carbon (gray) atoms are represented with 50% probability ellipsoids.

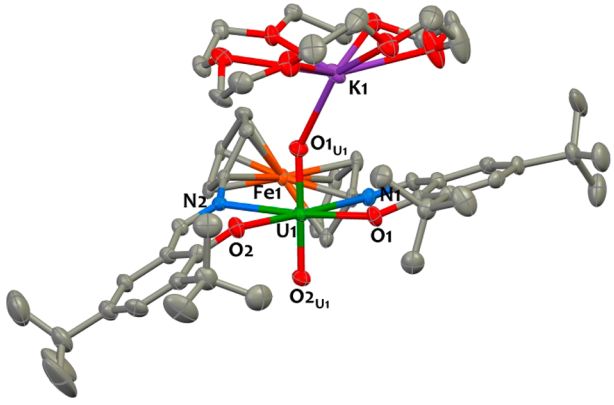

Figure 3. Solid-state molecular structure of the complex $[U_1O_2(salfen\text{-}^tBu_2)(K18\text{-}c\text{-}6)]$ in **2**. Hydrogen atoms and solvent molecules are omitted for clarity. Uranium (green), iron (orange), nitrogen (blue), potassium (purple), oxygen (red), and carbon (gray) atoms are represented with 50% probability ellipsoids.

the presence of two independent uranium complexes **U1** and **U2** in the asymmetric unit. Selected bond distances for **1** and **2** are given in Supporting Information, Table S.2. The coordination environment around the uranium center is similar in the two complexes. In compounds **1** and **2**, the uranium atoms are hexacoordinated in a tetragonal bipyramidal coordination geometry. The four donor atoms of the salfen-^{t}Bu$_2$ ligand (two oxygen and two nitrogen atoms) occupy the equatorial plane of the uranium ion (mean deviation from the plane of 0.04 Å in **1** and **U1**, of 0.06 Å in **U2**). The axial positions in **1** are occupied by two oxo ligands with U=O distances ranging between 1.831(4) and 1.864(4) Å and significantly longer than those found in the uranyl(VI) complex **1** (1.778(3) Å). These distances are in the range of those found in previously reported complexes of uranyl(V).[1d–f,11c,24] In the complexes **U1** and **U2** the $[K(18\text{-}c\text{-}6)]^+$ countercation binds one oxo group of the uranyl group through cation–cation interaction.[25] The K–O(1U1) distance (2.568(4) Å) is 0.2 Å smaller than K–O(1U2) (2.792(4) Å). This difference is probably because in **U2** the potassium ion interacts also with a phenolate oxygen (K–O = 2.941(4) Å) and an imino nitrogen (3.327(5) Å) from the Schiff base. The value of the distance between the uranium and iron atoms in complex **1** (3.708(1) Å) is smaller than the ones in **2** (mean distance 3.876(1) Å). This is the result of the presence of a stronger interaction of the ligand with the UO_2^{2+} cation resulting in shorter metal–ligand distances; notably, all the distances between the uranium ion and the ligand donor atoms in the equatorial plane are smaller by 0.1 Å in the uranyl(VI) complex compared to the uranyl(V) one (mean distances: U–O 2.221(3) Å, U–N 2.460(3) Å in **1** and U–O 2.31(1) Å, U–N 2.54(1) Å in **2**).

The above results show that the ferrocene-based salfen-^{t}Bu$_2$ ligand leads to stable complexes of uranyl(VI) and uranyl(V). We then become interested in studying the ability of these ligands to support uranium in lower oxidation states. In particular we have explored the possibility of obtaining homoleptic bis-ligand complexes of U(IV) with the objective of investigating the uranium-mediated communication between the two iron centers.[16b]

Tetravalent Uranium Salfen Complex. To favor the formation of a homoleptic bis-ligand complex of U(IV) the nonsubstituted salfen ligand was chosen to minimize steric hindrance. The salt metathesis reaction between $[UI_4(OEt_2)_2]$ and 2 equiv of the potassium salt of the tetradentate Schiff-base ligand K_2salfen in THF affords the homoleptic U(IV) complex $[U(salfen)_2]$ **3** in 75% yield (Scheme 3). The ^{1}H NMR spectra

Scheme 3. Synthesis of $[U(salfen)_2]$ 3

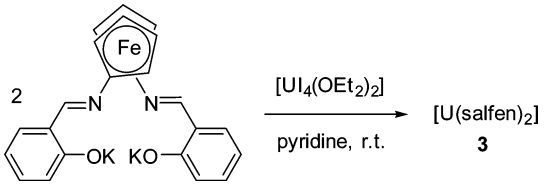

recorded for **3** in deuterated THF or pyridine show the presence of a single set of nine sharp resonances in agreement with the presence of a D_{2h} symmetric solution species.

Single crystals of **3** suitable for X-ray diffraction studies were grown by slow diffusion of diisopropyl ether into a THF solution of **3**. The solid-state structure of **3** is represented in Figure 4. The complex crystallizes in the monoclinic $P2_1/n$ space group. The uranium cation is encapsulated between two overlapping salfen ligands that provide a N_4O_4 coordination sphere around the metal. The resulting coordinating polyhedron around uranium is best described as a distorted square antiprism with N1–O1–N31–O31 and N2–O2–N32–O32 defining the square bases of the polyhedron. In the structures of the previously reported heteroleptic monoligand complexes $[Ce(salfen\text{-}^tBu_2)(O^tBu)_2]$[19] and $[Zr(salfen\text{-}^tBu_2)(CH_2Ph)_2]$,[17]

DOI: 10.1021/acs.inorgchem.5b00467
Inorg. Chem. 2015, 54, 5774–5783

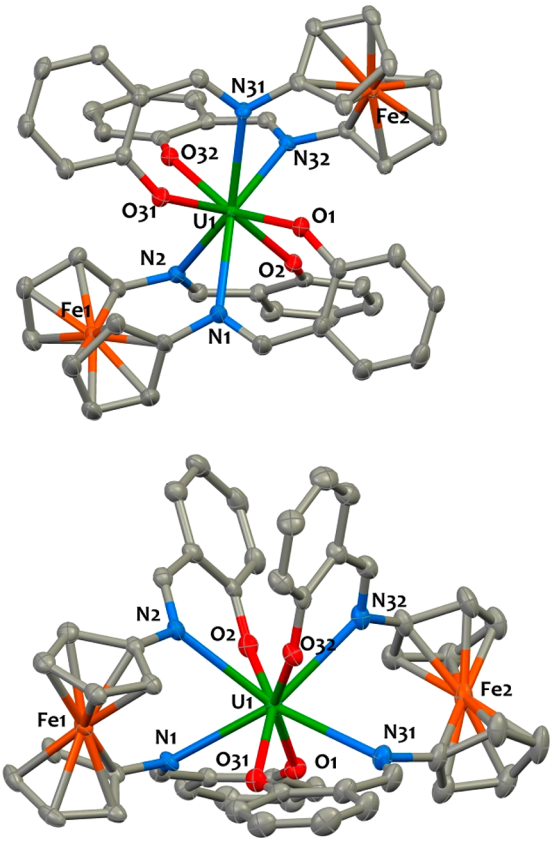

Figure 4. Two different views of the solid-state molecular structure of $[U(salfen)_2]$, **3**. Hydrogen atoms and solvent molecules are omitted for clarity. Uranium (green), iron (orange), nitrogen (blue), oxygen (red), and carbon (gray) atoms are represented with 50% probability ellipsoids. Selected metrical parameters are reported in Table 1.

as well as in **1** and **2**, the salfen ligand adopts a planar geometry. In contrast, in **3** the two N,O coordinating arms of the ligand are strongly twisted with respect to each other with an average angle of 73.7(7)° between the phenolate planes from the same ligand. This arrangement differs significantly from that found in the sandwich structure of the bis-ligand complex $[U(salophen)_2]$,[8a] highlighting the higher flexibility of the ferrocene Schiff base. The $U-O_{avg}$ 2.231(9) Å and $U-N_{avg}$ 2.664(7) Å bond distances are comparable to the ones in $[U(salophen)_2]$[8a] and fall in the range of those found in related uranium(IV) complexes.[13,26]

The two ferrocene units of the ligands are almost perpendicular, as indicated by the 71.3° value for the torsion angle between the Cp centroids and the irons in **3**. Both ferrocene moieties adopt roughly eclipsed conformations, with values of the N1−C1−C6−N2 and N31−C31−C36−N32 dihedral angles of 16.3(3)° and 15.7(2)°, respectively. The mean Fe−C distances 2.041(7) Å are close to those found in ferrocene.[27] The U···Fe separations (U1···Fe1 = 4.3087(5) Å ; U1···Fe2 = 4.3237(4) Å) have similar values for both ferrocene ligands. These values are longer than the ones (3.32 and 2.961 Å) respectively observed in the solid-state molecular structure of the related bis-diamidoferrocene complexes $[U(fc[NSiMe_3]_2)_2]$[28] and $[U(fc[NSi(t\text{-}Bu)Me_2]_2)_2][BPh_4]$.[16b] This is the result of the presence in the salfen ligand of imino groups with longer U−N distances, compared to the U−N distances in the diamidoferrocene complexes, which maintain the uranium further apart from the ferrocene.

Magnetic Data. The observed diamagnetism of compound **1** ($\chi = -4.62.10^{-3}$ emu·mol^{-1} at 300 K) is in agreement with the presence of a low-spin Fe(II) and a diamagnetic UO_2^{2+}. Temperature-dependent magnetic data for **2** and **3** were collected in the temperature range of 2−300 K. At 300 K, **2** displays an effective magnetic moment of 2.09 μ_B (Figure 5),

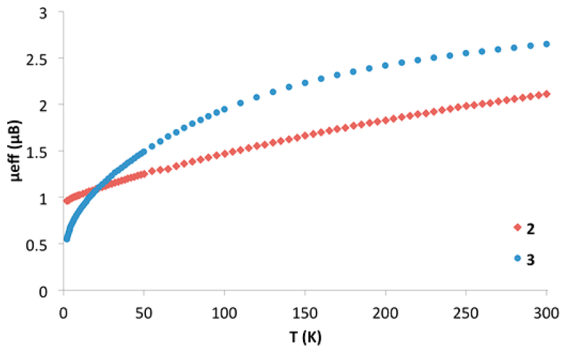

Figure 5. Temperature-dependent effective magnetic moment for **2** (red trace) and **3** (blue trace) recorded under 500 G in the range of 2−300 K. A μ_{eff} of 2.09 μ_B at 300 K was calculated for **2** ($\chi_{dia} = -7.44 \times 10^{-4}$ emu·mol^{-1}, m = 19.3 mg, Mw = 1291.4 g·mol^{-1}). A μ_{eff} of 2.64 μ_B at 300 K was calculated for **3** ($\chi_{dia} = -4.53 \times 10^{-4}$ emu·mol^{-1}, m = 24 mg, Mw = 1078.93 g·mol^{-1}).

which is in agreement with the presence of low-spin Fe(II) and U(V) ions. The magnetic moment of the U(V) ion is lower than the theoretical value calculated for the free $5f^1$ ion in the L−S coupling scheme ($\mu_{eff} = 2.54\ \mu_B$), but within the range of values reported for U^V compounds (1.42−2.57 μ_B).[29] The magnetic moment for **2** decreases with decreasing temperature and reaches 0.96 μ_B at 2 K, a behavior typically found in mononuclear uranyl(V) complexes.[11c]

In comparison, complex **3** exhibits a magnetic moment at 300 K of 2.64 μ_B, which falls in the typical range of values recorded for U(IV) complexes.[29] At low temperatures, the magnetic moment for **3** decreases drastically and tends to zero at 0 K, a behavior consistent with a singlet ground state as typically found for the f^2 uranium(IV) ion. A similar behavior had been reported for the U(IV) bis(1,1′-diamidoferrocene) complex $[U(fc[NSi(t\text{-}Bu)Me_2]_2)_2]$.[16b]

Redox Properties of Complexes 2 and 3. Complexes **2** and **3** possess three different types of redox-active centers: the uranium cation, the Fe(II) centers of the ferrocene units, and the imino moieties of the supporting ligand. To get more insight into the redox properties of these heterometallic complexes, cyclovoltammetric studies were performed. The measurements were performed on 2 mM pyridine solutions of complexes using $[Bu_4N][PF_6]$ as supporting electrolyte. The pyridine was used as solvent because of the instability of the uranyl(V) complex in THF. All redox potentials are referenced against the $[(C_5H_5)_2Fe]^{+/0}$ redox couple. The cyclovoltammetric study of K_2salfen-^{t}Bu$_2$ ligand show the presence of a redox event at $E_{1/2}$ = 0.24 V assigned to the Fe(II)/Fe(III) couple in the ferrocene spacer. This value compares well with the value measured for the H_2salfen-^{t}Bu$_2$ ligand in thf (0.29 V).[18]

Compound **2** exhibits a reversible event at $E_{1/2}$ = −1.61 V (Figure 6), which corresponds to a U(VI)/U(V) couple. The same reversible wave is observed in the voltammogram of **1** recorded using the same conditions. The value of the measured redox potential is very similar to that reported for

DOI: 10.1021/acs.inorgchem.5b00467
Inorg. Chem. 2015, 54, 5774−5783

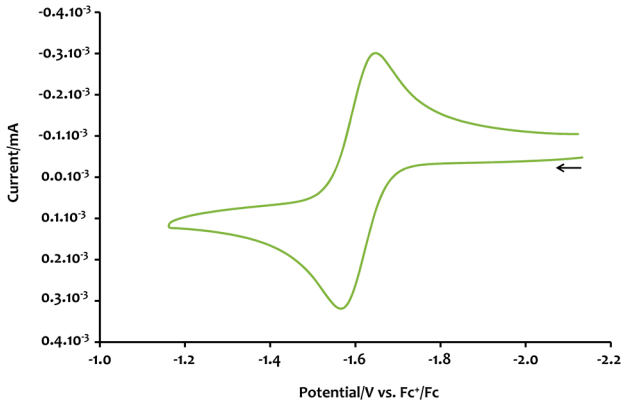

Figure 6. Room-temperature cyclic voltammogram for $[UO_2(salfen\text{-}^tBu_2)(K18\text{-}c\text{-}6)]$ **2** recorded in 0.1 M $[Bu_4N][PF_6]$ in 2 mM pyridine solution at 100 mV/s scan rate, Cp_2Fe/Cp_2Fe^+ corrected.

$[UO_2(salophen\text{-}^tBu_2)(Py)K]$,[11c] indicating that the degree of stabilization of the uranyl(V) cation is similar in both systems. Additionally, an irreversible oxidation wave is observed around 0.57 V with a shoulder at 0.34 V that can reasonably be assigned to the oxidation of the ligand ferrocene moiety. The high intensity of wave at 0.57 V suggests that further oxidation events might occur at this potential that might be assigned to the formation of ligand phenoxy radicals.

Complex **3** shows an irreversible reduction wave at E_{pc} = −2.49 V (Figure 7). This process is associated with several

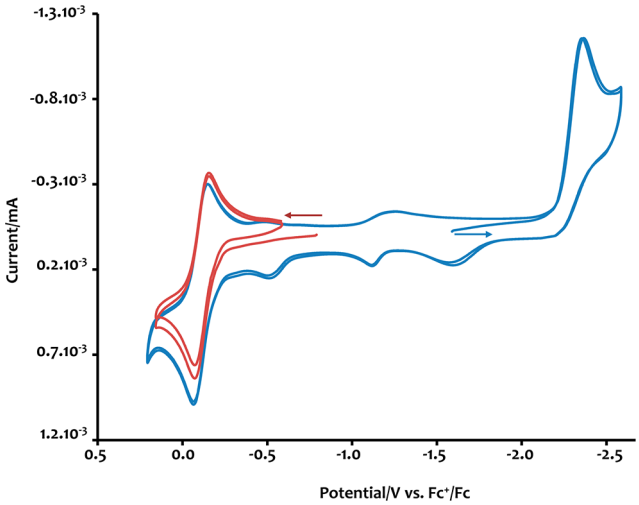

Figure 7. Room-temperature cyclic voltammograms for $[U(salfen)_2]$ **3** recorded in 0.1 M $[Bu_4N][PF_6]$ in 2 mM pyridine solution at 100 mV/s scan rate, Cp_2Fe/Cp_2Fe^+ corrected. The red trace corresponds to the voltammogram swept initially from −0.9 V to the positive direction, and the blue trace corresponds to the voltammogram swept initially from −1.5 V to the negative direction.

irreversible oxidation waves of lower intensity at E_{pa} = −1.54, −1.10, and −0.55 V, which are not observed when the voltammogram is swept initially from −2.0 V to the positive direction (Supporting Information, Figure S.23). On the basis of previous studies of the redox chemistry of f-elements bis-salophen complexes,[13,14b] this electrochemical signature is evocative of a reduction/oxidation feature involving the Schiff-base ligand, even if a U(IV)/U(III) process could also occur in this potential window.[16a] This process remains irreversible at higher scan-rate (5000 mV/s), suggesting that the electrochemically generated reduced species has a very short lifetime and undergoes rapid rearrangement/reaction. The multiple irreversible reoxidation waves indicate the formation of several products, which is in agreement with what is observed when the chemical reduction of **3** is performed (vide infra).

We also considered the electrochemical oxidation of $[U(salfen)_2]$, **3**. The cyclic voltammogram displays a reversible feature centered at $E_{1/2}$ = −0.14 V that is assigned to the Fe(II)/Fe(III) couple of the ferrocene moieties. Indeed, this potential is close to that of ferrocene and lies in between the values measured for the Fe^{2+}/Fe^{3+} oxidation in the monoligand complexes $[Ln(^{tBu}salfen)(O^tBu)(X)]$ ({Ln, X} = {Y, THF}: $E_{1/2}$ = 0.09 V; {Ln, X} = {Ce, O^{t}Bu}, $E_{1/2}$ = −0.28).[18] This indicates that the two chemically equivalent ferrocenes from the two Schiff-base ligands are oxidized at the same potential. Therefore, it is reasonable to assume that no iron−iron communication is occurring in **3**, which is consistent with the large U···Fe separation observed in the solid-state structure. Notably, systems in which an electronic communication occurs between two ferrocene units generally display two clearly distinct one-electron reversible waves.[16b,18,30]

Ligand-Centered Reduction. The ability of the salfen ligand to support uranium in a reduced form was also explored. The addition of 1 equiv of K_2salfen to a THF solution of $[UI_3(THF)_4]$ resulted in a rapid color change from deep blue to brown accompanied by the formation of KI precipitate. Analysis of the crude reaction mixture by ^{1}H NMR showed the formation of $[U(salfen)_2]$ **3** as the only salfen-containing species (Scheme 4).

Scheme 4. Reaction of $[UI_3(THF)_4]$ with K_2salfen

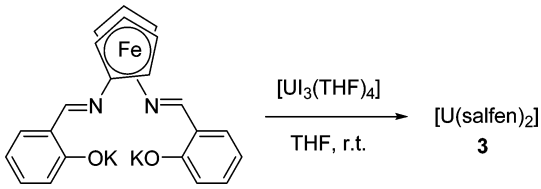

The uranium(IV) complex $[U(salfen)_2]$ is presumably formed by a disproportionation process yielding some form of U(0) that is removed by filtration. A similar behavior has been previously reported for various ligands when reacted with $[UI_3(THF)_4]$,[16c,26,31] including for the related bis(1,1′-diamidoferrocene) ligand $[K_2(OEt_2)_2]$fc[NSi-(*t*-Bu)Me$_2$]$_2$.[16b]

Overall, salt metathesis reactions of uranium iodides with salfen potassium salts underline that the salfen scaffold is able to stabilize and saturate the coordination sphere of a U(IV) ion but does not allow the synthesis of stable uranium(III) complexes.

Since previous studies on the related Schiff-base complex $[U(salophen)_2]$ have shown that further reduction of this complex was possible leading to the reduction of the imino group (Scheme 1), we decided to investigate the chemical reduction of compound **3**.

The reaction of **3** with 4 equiv of KC_8 per uranium atom in THF resulted in a color change of the solution from orange to dark brown. Analysis of the crude mixture by ^{1}H NMR revealed that a mixture of compounds was reproducibly obtained. The ^{1}H NMR spectrum recorded in deuterated THF for the crude reaction mixture displays a series of sharp resonances

DOI: 10.1021/acs.inorgchem.5b00467
Inorg. Chem. 2015, 54, 5774−5783

Scheme 5. Reduction of [U(salfen)$_2$] 3

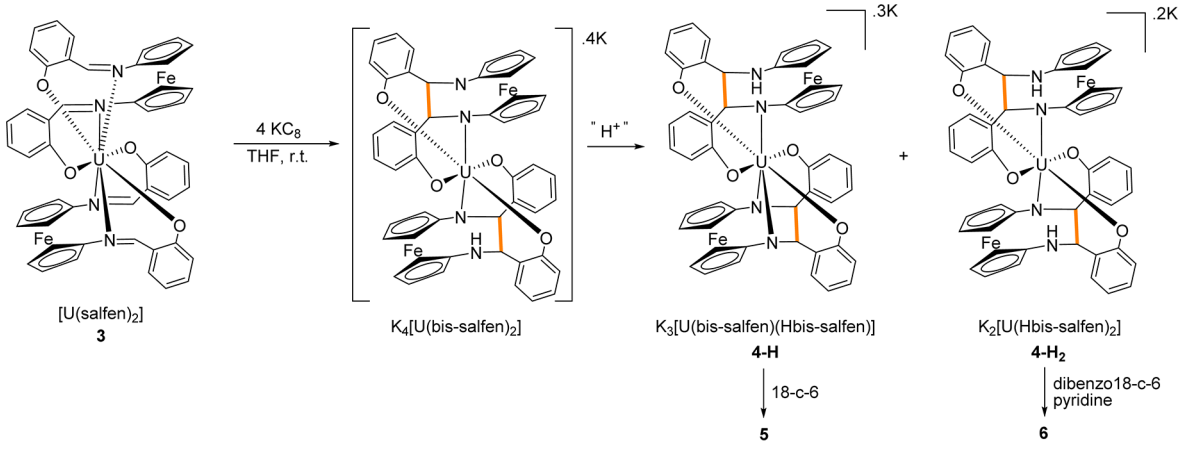

paramagnetically shifted in the +40 to −30 ppm range characteristic of U(IV) complexes.

A few crystals of the complex **4-H** (Scheme 5) could be grown by slow diffusion of diisopropylether in the crude mixture in THF. While the quality of the structure is not sufficient to allow for a detailed discussion of the metrical parameters of the structure, it is of reasonable quality to indicate atom connectivity. In the crystal structure of **4-H**, reported in Supporting Information, the uranium complexes K_3[U(bis-salfen)(Hbis-salfen)]·$(THF)_n$ (Figure 8) are connected in a one-dimensional coordination polymer by bridging potassium counter cations with different coordination modes and geometries (see Supporting Information, Figures S.18 and S.19). The ^{1}H NMR spectrum of **4-H** in THF-d_8 at 298 K features 36 sharp resonances over the range from 36.4 to −27.5 ppm. This shows the presence of fully asymmetric uranium(IV) solution species in agreement with the solid-state structure of this heteroleptic species. ESI/MS studies further support the formulation of **4-H** as K_3[U(bis-salfen)(Hbis-salfen)] in THF solution (m/z = 1201.0 corresponding to the {K_3[U(bis-salfen)(Hbis-salfen)]+H}$^+$ moiety).

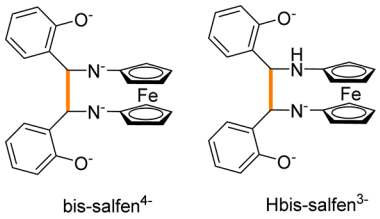

Figure 8. Drawing of the bis-salfen^{4-} and Hbis-salfen^{3-} ligands.

In presence of 18-c-6, the solid-state polymeric structure was disrupted, and single crystals of the dimer [(K18-c-6)$_2$U(bis-salfen)(Hbis-salfen)]$_2$(K18-c-6)$_2$·7thf, **5**, were obtained. X-ray diffraction studies show the presence of a centrosymmetric structure composed of two [(K18-c-6)U(bis-salfen)(Hbis-salfen)]$^{2-}$ moieties bridged by 2(K18-c-6)$^+$ units, as shown in Figure 9. The charge is balanced by two [K(18-c-6)]$^+$ countercations.

Selected metrical parameters are reported in Table 1. The uranium ion is heptacoordinated in a distorted capped trigonal prismatic arrangement. Upon reduction two new intramolecular C−C bonds formed between the imino moieties of each salfen ligand. This results in the formation of a new bisphenolate bisamido ligand (bis-salfen; Figure 8). The intraligand reductive coupling of the two imido moieties forms a linker between the two C_5H_5 ligands, yielding an *ansa*-ferrocene derivative. The structure shows that in one of the two bis-salfen ligands one amido group is protonated to give the Hbis-salfen ligand, which acts as a tridentate OON ligand, with the amino group (N32) remaining uncoordinated. The resulting heteroleptic complex is therefore composed of a

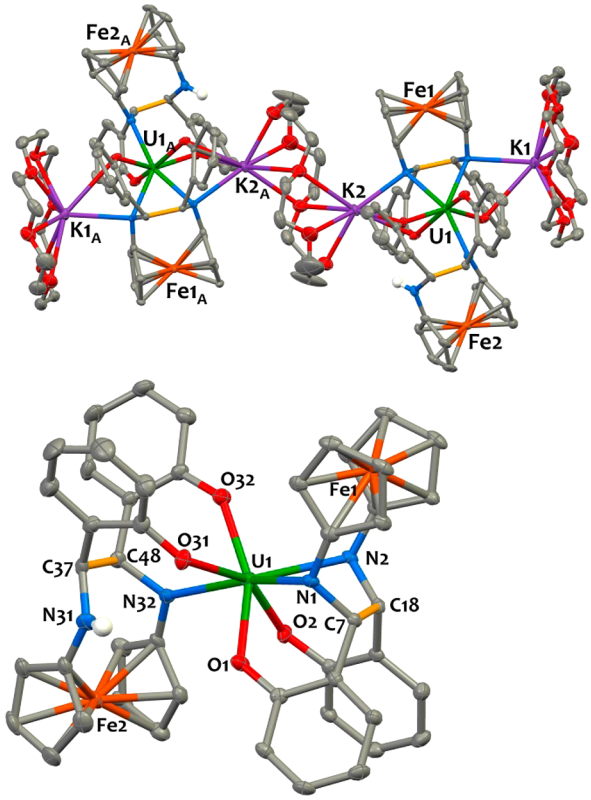

Figure 9. Ortep diagram of the solid-state molecular structure of the [(K18-c-6)$_2$U(bis-salfen)(Hbis-salfen)]$_2^{2-}$ dimeric anion in **5** (upper) and of the coordination environment around the uranium ion (lower). Hydrogen atoms, except that of the amino moiety, and interstitial solvent molecules are omitted for clarity. The C−C bonds formed by reduction of the imine moieties of the salfen ligands are represented in yellow. Uranium (green), iron (orange), nitrogen (blue), oxygen (red), potassium (purple), carbon (gray), and hydrogen (white) atoms are represented with 50% probability ellipsoids.

DOI: 10.1021/acs.inorgchem.5b00467
Inorg. Chem. 2015, 54, 5774−5783

Table 1. Mean Values of Selected Bond Lengths [Å] in the U(IV) Complexes 3, 5, and 6

compd	3	5	6
U−N	2.664(7)	2.46(6)	2.355(4)
U−O	2.231(9)	2.29(5)	2.24(3)
$C-C_{link}$		1.62(2)	1.586(8)
C−N	1.294(6)	1.471(3)	1.469(11)
U−Fe	4.316(11)	4.3450(2) (Fe1) 5.0419(3) (Fe2)	4.8874(9)
Fe−C	2.041(7)	2.046(17)	2.043(13)

U(IV) cation coordinated by a tetraanionic bis-salfen ligand and a trianionic Hbis-salfen ligand, which is consistent with the overall trianionic charge for the complex. The metrical parameters, given in Table 1, are in agreement with this description. Notably, the $U-N_{amido}$ average bond distance (2.46(6) Å) is shorter by ∼0.2 Å compared to the $U-N_{imino}$ bond distances found in **3** and falls in the range of what was observed in related U(IV) amido complexes.[8a,13] The C−N bond distances are elongated by ∼0.18 Å compared to those of complex **3**, in agreement with the reduction of the imine double C═N bond into amido/amino units.

Detailed analysis of the proton NMR spectrum of the reaction mixture obtained from the reduction of $[U(salfen)_2]$ with KC_8 reveals that this apparently complex pattern can be decomposed into two sets of resonances, one corresponding to the complex two **4-H** and one additional reduced complex with higher solution symmetry identified (see below) as $K_2[U(Hbis-salfen)_2]$ **4-H_2** (Scheme 5). However, their separation proved difficult, preventing the isolation of significant amounts of these species in analytically pure form.

Single crystals of $[K(dibenzo18-c-6)(Py)]_2[U(Hbis-salfen)_2]\cdot py_5$, **6**, were grown upon slow diffusion of hexane into a pyridine solution of the reaction mixture in the presence of dibenzo18-c-6. The solid-state structure consists of an isolated ion pair, and the structure of the $[U(Hbis-salfen)_2]^{2-}$ anion is presented in Figure 10. Selected bond distances are given in Table 1. The uranium(IV) cation lies on a symmetry center and

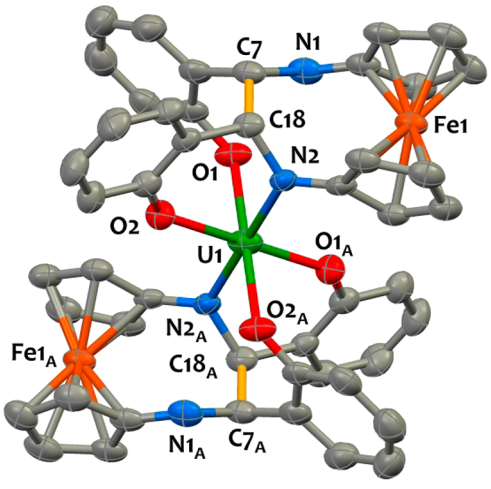

Figure 10. Solid-state molecular structure of the $[U(Hbis-salfen)_2]^{2-}$ anion in $[K(dibenzo18-c-6)(Py)]_2[U(Hbis-salfen)_2]\cdot py_5$ **6**. Hydrogen atoms and solvent molecules are omitted for clarity. The C−C bond formed through the reductive coupling of the imino groups is represented in yellow and uranium (green), nitrogen (blue), oxygen (red), iron (orange) ellipsoids. Selected metrical parameters are reported in Table 1

exhibits a pseudo-octahedral coordination with four phenolate moieties from the Hbis-salfen ligands coordinated in the equatorial plane and two amido moieties bound in a trans configuration. The NMR pattern of **4-H_2** features 18 signals, indicating that the ligands are equivalents on the NMR time scale in agreement with the ligand arrangement found in the solid-state crystal structure of **6**. The value of the distance of the C−C bond formed from the coupling of two imino groups is 1.586(8) Å. The value of the C−C bond distance falls in the range of the ones found in bis-salophen, cyclo-salophen, and bis-napthquinolen ligands formed from reductive coupling of imino groups in tetradentate and tridentate Schiff bases, respectively.[8a,13] Similarly to **5**, the C18−N2 and C7−N1 bond distances (1.476(6) Å and 1.461(5) Å) in **6** are longer than the $C-N_{imino}$ bond distances found in **3** and correspond to C−N simple bonds. The U1−N2 bond distance (2.355(4) Å) is much shorter than the $U-N_{imino}$ bond distances found in **3**, which is consistent with an amido moiety. While N2 is coordinated to the uranium cation, as expected for an amido moiety, the neutral amino nitrogen N1 remains uncoordinated to the metal center. The average value of the U−O bond distances (2.24(3) Å) is in line with those reported for U(IV) phenolate systems.[8a,26] The U···Fe separation (4.8874(9) Å) in **6** is longer than the one in **3**. Finally, the overall K/U ratio is 2, in agreement with a +IV charge for the uranium. Thus, the formula $[U(Hbis-salfen)_2]^{2-}$ where Hbis-salfen is a trianionic tridentate ligand provides a good description of the complex.

These studies indicate that ligand reduction is more favorable than a U(IV) to U(III) process. The complex reduction results in the reductive coupling of the imino moieties of the salfen ligand yielding U(IV) amidophenolate compounds. Metal-mediated intramolecular and intermolecular reductive coupling of the imino group of the tetradentate Schiff-base salophen has been previously reported for U(IV) (Scheme 1),[8a] Ln(III),[14b] and d-block metals.[32] However, the isolated complexes **4-H** and **4-H_2** show that in the reduction of the $[U(salfen)_2]$ complex, the reductive coupling occurs between the imino groups of the same salfen ligand (Scheme 5). Such reactivity is unprecedented, and it is most likely the result of the higher flexibility of the salfen ligand compared to the salophen one.

Mixtures of **4-H** and **4-H_2** were reproducibly obtained from independent syntheses. These species are, respectively, the monoprotonated and the diprotonated analogues of a bis-amido bis-phenolate $[U(bis-salfen)_2]^{4-}$ complex and are probably formed by hydrogen abstraction from the solvent. We previously observed that the amido moieties of the bis-salophen ligand formed upon reductive coupling of the salophen Schiff-base feature a basic character.[14b] In the putative tetraanionic mononuclear $[U(bis-salfen)_2]^{4-}$ species (Scheme 5), resulting from the four-electron reduction of $[U(salfen)_2]$, the octaanionic environment provided at the U(IV) cation by the four phenolates and four amido groups likely results in a high electron density at the metal responsible for the low stability of this species. Unfortunately, efforts to characterize this intermediate so far proved unsuccessful in our hands. Attempts to perform the reduction in the more robust 1,2-dimethoxyethane solvent afforded the same mixture of compounds. Similar results were obtained when replacing KC_8 by K metal. Using a larger number of equivalents of potassium graphite resulted in the formation of intractable mixtures containing **4-H_2** and/or **4-H** together with other unidentified reduction products. When only 2 equiv of KC_8 are

DOI: 10.1021/acs.inorgchem.5b00467
Inorg. Chem. 2015, 54, 5774−5783

used in the reduction, a mixture of unreacted complex **3** and reduced **4-H** and **4-H$_2$** species were obtained.

Interestingly, preliminary studies show that despite the presence of protonated amino groups the electrons stored in the C−C bonds can became available to oxidizing agents. Notably, the addition of 4 equiv of AgOTf to the reaction mixture of **4-H** and **4-H$_2$** led to immediate restoration of the original [U(salfen)$_2$] (Scheme 6). This suggests that the

Scheme 6

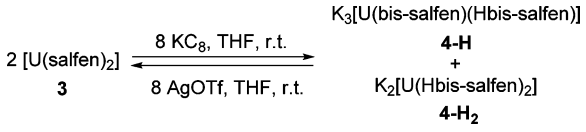

[U(salfen)$_2$] can be used to store four electrons for the reduction of substrates even in the presence of proton sources. This result contrasts with what was previously found for the complex K[Nd(bis-H$_2$salophen)] where the electrons stored in the C−C bond of the protonated bis-salophen ligand are no longer available to oxidizing agents.[14b] Work in progress is directed to investigate the reactivity of the reduced [U(salfen)$_2$] and to probe its ability to transfer the electrons stored in the C−C bond to different oxidizing substrates.

CONCLUSIONS

In summary, a series of heterometallic uranium−iron complexes was synthesized and fully characterized by NMR spectroscopy, single-crystal X-ray diffraction, variable-temperature magnetic measurements, and cyclovoltammetry. The ferrocene-based Schiff-base ligand salfen was shown to be a good platform for stabilizing the three higher oxidation states of uranium (IV, V, and VI). The reduction of the U(IV) bis-ligand complex [U(salfen)$_2$] led to ligand-centered reduction involving the reductive coupling of the imino groups on the Schiff-base ligand. This results in the unprecedented formation of an intramolecular intraligand C−C bond between the two imino groups of a salfen ligand rather than in the interligand C−C bond formation reported previously for tridentate and tetradentate Schiff bases. Such novel reactivity arises from the high flexibility of the ferrocene backbone. We also show that the electrons stored in the C−C bond are available for the oxidation of substrates. Future work will be directed to investigate the reactivity of the reported complexes.

ASSOCIATED CONTENT

Supporting Information

Synthesis information, selected ^{1}H NMR spectra, electrochemistry and magnetism data, and X-ray crystallographic data and files in CIF format. This material is available free of charge via the Internet at http://pubs.acs.org.

AUTHOR INFORMATION

Corresponding Author

*E-mail: marinella.mazzanti@epfl.ch.

Author Contributions

All authors have given approval to the final version of the manuscript.

Notes

The authors declare no competing financial interest.

ACKNOWLEDGMENTS

We thank Stephanie M. Quan and Prof. P. Diaconescu for kindly giving us generous samples of the salfen ligands. We thank C. Lebrun, J.-F. Jaquot, J. Hermle, and P.-A. Bayle for their contribution to the spectroscopic characterizations.

REFERENCES

(1) (a) Graves, C. R.; Kiplinger, J. L. *Chem. Commun.* **2009**, 3831−3853. (b) Graves, C. R.; Scott, B. L.; Morris, D. E.; Kiplinger, J. L. *J. Am. Chem. Soc.* **2007**, *129*, 11914−11915. (c) Arnold, P. L.; Love, J. B.; Patel, D. *Coord. Chem. Rev.* **2009**, *253*, 1973−1978. (d) Natrajan, L.; Burdet, F.; Pecaut, J.; Mazzanti, M. *J. Am. Chem. Soc.* **2006**, *128*, 7152−7153. (e) Hayton, T. W.; Wu, G. *J. Am. Chem. Soc.* **2008**, *130*, 2005−2014. (f) Nocton, G.; Horeglad, P.; Pecaut, J.; Mazzanti, M. *J. Am. Chem. Soc.* **2008**, *130*, 16633−16645.

(2) (a) MacDonald, M. R.; Fieser, M. E.; Bates, J. E.; Ziller, J. W.; Furche, F.; Evans, W. J. *J. Am. Chem. Soc.* **2013**, *135*, 13310−13313. (b) Arnold, P. L.; Patel, D.; Wilson, C.; Love, J. B. *Nature* **2008**, *451*, 315−318. (c) La Pierre, H. S.; Scheurer, A.; Heinemann, F. W.; Hieringer, W.; Meyer, K. *Angew. Chem., Int. Ed.* **2014**, *53*, 7158−7162.

(3) (a) King, D. M.; Liddle, S. T. *Coord. Chem. Rev.* **2014**, *266*, 2−15. (b) La Pierre, H. S.; Meyer, K. In *Progress in Inorganic Chemistry;* Karlin, K. D.; Ed. **2014**; Vol. *58*, pp 303−415. (c) Arnold, P. L. *Chem. Commun.* **2011**, *47*, 9005−9010. (d) Summerscales, O. T.; Cloke, F. G. N.; Hitchcock, P. B.; Green, J. C.; Hazari, N. *Science* **2006**, *311*, 829−831. (e) Frey, A. S. P.; Cloke, F. G. N.; Coles, M. P.; Maron, L.; Davin, T. *Angew. Chem., Int. Ed.* **2011**, *50*, 6881−6883. (f) Thomson, R. K.; Cantat, T.; Scott, B. L.; Morris, D. E.; Batista, E. R.; Kiplinger, J. L. *Nat. Chem.* **2010**, *2*, 723−729. (g) King, D. M.; Tuna, F.; McInnes, E. J. L.; McMaster, J.; Lewis, W.; Blake, A. J.; Liddle, S. T. *Science* **2012**, *337*, 717−720. (h) Karmel, I. S. R.; Fridman, N.; Tamm, M.; Eisen, M. S. *J. Am. Chem. Soc.* **2014**, *136*, 17180−17192. (i) Camp, C.; Pecaut, J.; Mazzanti, M. *J. Am. Chem. Soc.* **2013**, *135*, 12101−12111.

(4) Nocton, G.; Pecaut, J.; Mazzanti, M. *Angew. Chem., Int. Ed.* **2008**, *47*, 3040−3042.

(5) (a) Layfield, R. A. *Organometallics* **2014**, *33*, 1084−1099. (b) Long, J. R.; Meihaus, K. R. *J. Chem. Soc., Dalton Trans.* **2015**, *44*, 2517−2528.

(6) (a) Rinehart, J. D.; Long, J. R. *J. Am. Chem. Soc.* **2009**, *131*, 12558−12559. (b) Mougel, V.; Chatelain, L.; Pecaut, J.; Caciuffo, R.; Colineau, E.; Griveau, J. C.; Mazzanti, M. *Nat. Chem.* **2012**, *4*, 1011−1017. (c) Pereira, L. C. J.; Camp, C.; Coutinho, J. T.; Chatelain, L.; Maldivi, P.; Almeida, M.; Mazzanti, M. *Inorg. Chem.* **2014**, *53*, 11809−11811.

(7) Sessler, J. L.; Melfi, P. J.; Pantos, G. D. *Coord. Chem. Rev.* **2006**, *250*, 816−843.

(8) (a) Camp, C.; Mougel, V.; Horeglad, P.; Pecaut, J.; Mazzanti, M. *J. Am. Chem. Soc.* **2010**, *132*, 17374−17377. (b) Salmon, L.; Thuery, P.; Ephritikhine, M. *J. Chem. Soc., Dalton Trans.* **2004**, 4139−4145. (c) Salmon, L.; Thuery, P.; Ephritikhine, M. *J. Chem. Soc., Dalton Trans.* **2004**, 1635−1643. (d) Arnold, P. L.; Potter, N. A.; Carmichael, C. D.; Slawin, A. M. Z.; Roussel, P.; Love, J. B. *Chem. Commun.* **2010**, *46*, 1833−1835.

(9) Arnold, P. L.; Stevens, C. J.; Farnaby, J. H.; Gardiner, M. G.; Nichol, G. S.; Love, J. B. *J. Am. Chem. Soc.* **2014**, *136*, 10218−10221.

(10) Arnold, P. L.; Potter, N. A.; Magnani, N.; Apostolidis, C.; Griveau, J. C.; Colineau, E.; Morgenstern, A.; Caciuffo, R.; Love, J. B. *Inorg. Chem.* **2010**, *49*, 5341−5343.

(11) (a) Mizuoka, K.; Tsushima, S.; Hasegawa, M.; Hoshi, T.; Ikeda, Y. *Inorg. Chem.* **2005**, *44*, 6211−6218. (b) Takao, K.; Tsushima, S.; Takao, S.; Scheinost, A. C.; Bernhard, G.; Ikeda, Y.; Hennig, C. *Inorg. Chem.* **2009**, *48*, 9602−9604. (c) Mougel, V.; Horeglad, P.; Nocton, G.; Pecaut, J.; Mazzanti, M. *Angew. Chem., Int. Ed.* **2009**, *48*, 8477−8480. (d) Mougel, V.; Horeglad, P.; Nocton, G.; Pecaut, J.; Mazzanti, M. *Chem.—Eur. J.* **2010**, *16*, 14365−14377. (e) Nocton, G.; Horeglad, P.; Vetere, V.; Pecaut, J.; Dubois, L.; Maldivi, P.; Edelstein, N. M.; Mazzanti, M. *J. Am. Chem. Soc.* **2010**, *132*, 495−508. (f) Mougel, V.; Pecaut, J.; Mazzanti, M. *Chem. Commun.* **2012**, *48*, 868−870.

DOI: 10.1021/acs.inorgchem.5b00467
Inorg. Chem. 2015, 54, 5774−5783

(g) Mougel, V.; Horeglad, P.; Nocton, G.; Pecaut, J.; Mazzanti, M. *Chem.—Eur. J.* **2010**, *16*, 14365−14377.
(12) (a) Mougel, V.; Chatelain, L.; Hermle, J.; Caciuffo, R.; Colineau, E.; Tuna, F.; Magnani, N.; de Geyer, A.; Pecaut, J.; Mazzanti, M. *Angew. Chem., Int. Ed.* **2014**, *53*, 819−823. (b) Chatelain, L.; Walsh, J. P. S.; Pecaut, J.; Tuna, F.; Mazzanti, M. *Angew. Chem., Int. Ed.* **2014**, *53*, 13434−13438.
(13) Camp, C.; Andrez, J.; Pecaut, J.; Mazzanti, M. *Inorg. Chem.* **2013**, *52*, 7078−7086.
(14) (a) Cozzi, P. G. *Chem. Soc. Rev.* **2004**, *33*, 410−421. (b) Camp, C.; Guidal, V.; Biswas, B.; Pecaut, J.; Dubois, L.; Mazzanti, M. *Chem. Sci.* **2012**, *3*, 2433−2448.
(15) Diaconescu, P. L. *Comments Inorg. Chem.* **2010**, *31*, 196−241.
(16) (a) Duhovic, S.; Oria, J. V.; Odoh, S. O.; Schreckenbach, G.; Batista, E. R.; Diaconescu, P. L. *Organometallics* **2013**, *32*, 6012−6021. (b) Monreal, M. J.; Carver, C. T.; Diaconescu, P. L. *Inorg. Chem.* **2007**, *46*, 7226−7228. (c) Monreal, M. J.; Diaconescu, P. L. *Organometallics* **2008**, *27*, 1702−1706. (d) Monreal, M. J.; Diaconescu, P. L. *J. Am. Chem. Soc.* **2010**, *132*, 7676−7683. (e) Monreal, M. J.; Khan, S.; Diaconescu, P. L. *Angew. Chem., Int. Ed.* **2009**, *48*, 8352−8355. (f) Monreal, M. J.; Khan, S. I.; Kiplinger, J. L.; Diaconescu, P. L. *Chem. Commun.* **2011**, *47*, 9119−9121. (g) Diaconescu, P. L. *Acc. Chem. Res.* **2010**, *43*, 1352−1363. (h) Shafir, A.; Arnold, J. *J. Am. Chem. Soc.* **2001**, *123*, 9212−9213. (i) Ramos, A.; Otten, E.; Stephan, D. W. *J. Am. Chem. Soc.* **2009**, *131*, 15610−15611. (j) Green, A. G.; Kiesz, M. D.; Oria, J. V.; Elliott, A. G.; Buechler, A. K.; Hohenberger, J.; Meyer, K.; Zink, J. I.; Diaconescu, P. L. *Inorg. Chem.* **2013**, *52*, 5603−5610. (k) Huang, W.; Dulong, F.; Khan, S. I.; Cantat, T.; Diaconescu, P. L. *J. Am. Chem. Soc.* **2014**, *136*, 17410−17413. (l) Wang, X.; Thevenon, A.; Brosmer, J. L.; Yu, I.; Khan, S. I.; Mehrkhodavandi, P.; Diaconescu, P. L. *J. Am. Chem. Soc.* **2014**, *136*, 11264−11267.
(17) Shafir, A.; Fiedler, D.; Arnold, J. *J. Chem. Soc., Dalton Trans.* **2002**, 555−560.
(18) Broderick, E. M.; Thuy-Boun, P. S.; Guo, N.; Vogel, C. S.; Sutter, J.; Miller, J. T.; Meyer, K.; Diaconescu, P. L. *Inorg. Chem.* **2011**, *50*, 2870−2877.
(19) Broderick, E. M.; Diaconescu, P. L. *Inorg. Chem.* **2009**, *48*, 4701−4706.
(20) Carmichael, C. D.; Jones, N. A.; Arnold, P. L. *Inorg. Chem.* **2008**, *47*, 8577−8579.
(21) Avens, L. R.; Bott, S. G.; Clark, D. L.; Sattelberger, A. P.; Watkin, J. G.; Zwick, B. D. *Inorg. Chem.* **1994**, *33*, 2248−2256.
(22) *CrysAlisPro CCD; CrysAlisPro RED ; ABSPACK; CrysAlis PRO;* Agilent Technologies: Yarnton, England, 2010.
(23) Horeglad, P.; Nocton, G.; Filinchuk, Y.; Pecaut, J.; Mazzanti, M. *Chem. Commun.* **2009**, 1843−1845.
(24) Chatelain, L.; Mougel, V.; Pecaut, J.; Mazzanti, M. *Chem. Sci.* **2012**, *3*, 1075−1079.
(25) (a) Burdet, F.; Pecaut, J.; Mazzanti, M. *J. Am. Chem. Soc.* **2006**, *128*, 16512−16513. (b) Krot, N. N.; Grigoriev, M. S. *Russ. Chem. Rev.* **2004**, *73*, 89−100.
(26) Mora, E.; Maria, L.; Biswas, B.; Camp, C.; Santos, I.; Pécaut, J.; Cruz, A.; Carretas, J. M.; Marçalo, J.; Mazzanti, M. *Organometallics* **2013**, *32*, 1409−1422.
(27) Dunitz, J. D.; Orgel, L. E.; Rich, A. *Acta Crystallogr.* **1956**, *9*, 373−375.
(28) Westmoreland, I.; Arnold, J. *Acta Crystallogr., Sect. E* **2006**, *62*, M2303−M2304.
(29) Kindra, D. R.; Evans, W. J. *Chem. Rev.* **2014**, *114*, 8865−8882.
(30) Kaufmann, L.; Breunig, J.-M.; Vitze, H.; Schoedel, F.; Nowik, I.; Pichlmaier, M.; Bolte, M.; Lerner, H.-W.; Winter, R. F.; Herber, R. H.; Wagner, M. *J. Chem. Soc., Dalton Trans.* **2009**, 2940−2950.
(31) (a) Yin, H.; Lewis, A. J.; Williams, U. J.; Carroll, P. J.; Schelter, E. J. *Chem. Sci.* **2013**, *4*, 798−805. (b) Odom, A. L.; Arnold, P. L.; Cummins, C. C. *J. Am. Chem. Soc.* **1998**, *120*, 5836−5837. (c) Baker, R. J. *Coord. Chem. Rev.* **2012**, *256*, 2843−2871. (d) Chomitz, W. A.; Minasian, S. G.; Sutton, A. D.; Arnold, J. *Inorg. Chem.* **2007**, *46*, 7199−7209. (e) Lewis, A. J.; Williams, U. J.; Kikkawa, J. M.; Carroll, P. J.; Schelter, E. J. *Inorg. Chem.* **2012**, *51*, 37−39. (f) Duhovic, S.; Khan, S.; Diaconescu, P. L. *Chem. Commun.* **2010**, *46*, 3390−3392.
(32) (a) Gambarotta, S.; Mazzanti, M.; Floriani, C.; Zehnder, M. *J. Chem. Soc., Chem. Commun.* **1984**, 1116−1118. (b) Solari, E.; Maltese, C.; Franceschi, F.; Floriani, C.; ChiesiVilla, A.; Rizzoli, C. *J. Chem. Soc., Dalton Trans.* **1997**, 2903−2910.

DOI: 10.1021/acs.inorgchem.5b00467
Inorg. Chem. 2015, 54, 5774−5783